Electronic transport in the ferromagnetic pyrochlore Lu_{2}V_{2}O_{7}: Role of magnetization

Xiaohang Zhang, Haidong Zhou, Liuqi Yu, H. Jeffery Gardner, Stephan von Molnár, Christopher Wiebe, and Peng Xiong

Phys. Rev. B **91**, 205107 — Published 8 May 2015
DOI: 10.1103/PhysRevB.91.205107

Electronic Transport in the Ferromagnetic Pyrochlore $Lu_2V_2O_7$: the Role of Magnetization

Xiaohang Zhang,[1,†] Haidong Zhou,[2,3] Liuqi Yu,[1] H. Jeffery Gardner,[1] Stephan von Molnár,[1]
Christopher Wiebe,[4] and Peng Xiong[1]

[1]*Department of Physics, Florida State University, Tallahassee, Florida 32306*

[2]*National High Magnetic Field Laboratory, Tallahassee, Florida 32310*

[3]*Department of Physics & Astronomy, University of Tennessee, Knoxville, TN 37996*

[4]*Department of Chemistry, University of Winnipeg, Winnipeg, MB, R3B 2E9 Canada*

[†]*present address: Department of Materials Science and Engineering & Center for Nanophysics and Advanced Materials, University of Maryland, College Park, Maryland 20742*

ABSTRACT This work reports on a study of the resistivity and Hall effect of the ferromagnetic pyrochlore $Lu_2V_2O_7$. The temperature dependence of the resistivity of single crystalline $Lu_2V_2O_7$ exhibits overall activation behavior with a metallic-like exception at intermediate temperatures near the T_C. It is interesting to note that this temperature dependence bears a surprising resemblance to that of doped semiconductors. The ferromagnetic oxide shows a negative magnetoresistance which scales quadratically with the reduced magnetization at temperatures above the T_C; however, the scaling factor is significantly smaller than the value expected for a ferromagnetic system in the pure spin scattering regime, suggesting that other scattering processes may be at work. Concomitant with the negative magnetoresistance, a distinct switch in the Hall resistivity slope is observed at temperatures near the T_C. Our analysis suggests that the nonlinear Hall effect is associated with a change in the effective carrier density at a constant critical magnetization induced by an external magnetic field. We argue that within a picture that incorporates high-temperature activation transport with a magnetization-driven charge percolation transition, the observed complex electronic transport in the ferromagnetic pyrochlore can be quantitatively described.

PACS numbers: 75.50.Pp, 72.20.-i, 72.20.Pa, 72.20.Jv

In recent years, materials with a pyrochlore structure ($A_2B_2O_7$, where A and B ions form a network of corner-linked tetrahedra) have attracted great interest because the local spins in these systems give rise to many novel properties [1,2]. For example, with large magnetic moments on the A-site and strong crystal field effects, a disordered state known as a spin-ice can be stabilized on this lattice [3-8]. It is suggested that this unusual local-spin configuration is responsible for many emergent phenomena observed in these magnetically-frustrated systems. For instance, an unconventional anomalous Hall effect (AHE) observed in many pyrochlore materials [6-8] has been ascribed to the spin chirality of the spin-ice state while evidence of magnetic monopoles in these systems has also been recently reported [9,10]. Another interesting discovery in pyrochlore systems is the large negative magnetoresistance (MR) observed in the metallic ferromagnet $Tl_2Mn_2O_7$ [11,12]. Such a significant drop in resistance with applied magnetic field has been previously observed in mixed-valence manganites [13-15], which is now widely known as colossal magnetoresistance (CMR). It was believed that the CMR and the metal-insulator transition in mixed-valence manganites are closely related to the double exchange between Mn^{4+} and Mn^{3+} ions and the Jahn-Teller distortion of MnO_6 octahedra through the ferromagnetic transition. However, in the stoichiometric $Tl_2Mn_2O_7$, such a structural distortion is unlikely but the observed negative MR is quantitatively similar to the CMR in mixed-valence manganites. Specifically, it has been demonstrated that the MR of many ferromagnets with low carrier densities, including $Tl_2Mn_2O_7$ and many mixed-valence manganites, depends quadratically on the magnetization in the paramagnetic phase [16-22]. In addition, it has been found that the negative MR in these magnetic systems is always accompanied by a change in the Hall resistivity slope [23-29] which suggests a change in the effective carrier density with the applied magnetic field. A recent work [28] indicates that the observed nonlinear Hall effect (HE) in magnetic materials is a signature of a percolative transition occurring at a critical magnetization.

Recently, a large negative MR associated with a ferromagnetic transition in the pyrochlore $Lu_2V_2O_7$ was reported [30]. Although the MR of the material is similar to that observed in $Tl_2Mn_2O_7$ and mixed-valence manganites, $Lu_2V_2O_7$ shows a distinct non-metallic ferromagnetic state at low temperature. Therefore, the material provides a special and important model system for the study of the correlation between local moments and charge carriers in magnetic systems.

In this report, we present a systematic study of the electronic transport of $Lu_2V_2O_7$ single crystals. Specifically, to reveal the role of magnetization in the observed unusual transport behavior, we directly investigated the interplay of the magnetization and the charge carrier density in the material. Our analysis based on the MR and the magnetization suggests that the small magnetic-polaron hopping model [31-39] alone cannot provide a complete explanation for the high-temperature activation behavior observed in $Lu_2V_2O_7$. Moreover, our studies on the dramatic change in the Hall resistivity slope at temperatures near the T_C (69.5 K) suggest that a magnetization-driven percolative transition of *d*-band impurity states occurs at a characteristic magnetization. We argue that freeze-out of the in-gap states leads to the non-metallic ground state for the ferromagnetic semiconductor $Lu_2V_2O_7$.

$Lu_2V_2O_7$ single crystals used in this study were grown by the traveling-solvent floating-zone technique [30]. MR and HE measurements were performed in a JANIS ^{4}He cryostat with a 8-tesla superconducting magnet. Fig. 1a shows the temperature dependence of the resistivity measured on a 3.45mm × 2.35mm × 0.18mm platelet at zero and 8 T magnetic field, respectively. Consistent with the previous observation [30], the results show a large negative MR in the temperature range near the T_C. Plotting the resistivity as a function of the inverse of temperature, as in the inset of Fig. 1a, reveals explicitly three distinct temperature ranges with two activated regions (A and C) separated by a metallic one (B) at intermediate temperatures. Similar to the mixed-valence manganites, $Lu_2V_2O_7$ shows a metal-insulator-like transition at a temperature near the T_C. At high temperatures, it has been suggested that the activation behavior in many ferromagnetic materials [31-39] is governed by the adiabatic or the non-adiabatic polaron hopping mechanism described by

$$\rho = \rho_0 T^n \exp\left(\frac{E_\rho}{k_B T}\right) \tag{1}$$

with $n = 1$ for adiabatic polaron hopping and $n = 3/2$ for non-adiabatic polaron hopping. Here, k_B is the Boltzmann constant, T is the temperature, ρ_0 is a resistivity constant, and E_ρ is the activation energy. For the electronic transport of $Lu_2V_2O_7$ in the high temperature activated region from 75 K to 200 K, the best fits to the adiabatic polaron hopping model ($E_\rho = 54meV$) and the non-adiabatic polaron hopping model ($E_\rho = 57meV$), respectively, are shown in Fig. 1b. As a comparison, a fit to the simple Arrhenius activation ($n = 0$ in Eq. 1) in the same temperature range is also plotted in the figure, which yields an activation energy $E_\rho = 43meV$. In addition, previous study also suggested that the Mott variable-range hopping (VRH) model might be applicable to high-temperature transport of the material [x]. However, apparently, there is no significant difference in terms of the fitting quality for these models, which makes it difficult to definitively determine the transport mechanism in $Lu_2V_2O_7$ based on the activation analysis alone.

Besides the activation behavior as in Eq. 1, another well-established characteristic for the small magnetic-polaron hopping mechanism is the scaling of the MR with magnetization. It has been known for decades that the low-field MR in many ferromagnetic materials scales with the square of the reduced magnetization [16-22], following

$$\Delta\rho / \rho \approx C\left(M / M_{sat}\right)^2 \tag{2}$$

where M is the magnetization of the system, M_{sat} is the saturation magnetization and C is a scaling constant. Based on the Born approximation, Majumdar and Littlewood [22] further suggested that in materials where electron scattering from magnetic fluctuations is the major component of the electrical resistivity, the scaling constant C approximately equals to $x^{-2/3}$ with x representing the number of charge carriers per magnetic unit cell. This simple relation has been verified on a number of low-carrier-density ferromagnetic materials where spin scattering is expected to be predominant [22,40-45]. In contrast, although the quadratic scaling (Eq. 2) may still hold for materials with *competing* processes, the scaling factor C in these systems is no longer necessarily correlated with x. For instance, the actual scaling factor C is about two orders of magnitude higher than $x^{-2/3}$ for the ferromagnetic semimetal EuB_6 [46] in which, with the holes localized in magnetic polarons, the transport in the paramagnetic phase is dominated by itinerant electrons [27,28]. Another notable exception is slightly-doped perovskite manganites. Although it is believed that the high-temperature electronic transport is mainly through magnetic polaron hopping, the MR and the magnetization of perovskite manganites with a Mn^{4+} density less than 0.2 per unit cell show evident deviation from the simple scaling law [22] presumably due to the strong interaction between the charge carriers and the lattice [47-50].

To have a better understanding of the scattering mechanism in $Lu_2V_2O_7$, we performed a systematic study on the correlation between the observed MR and the magnetization of the material. Fig. 2a shows the MR at selected temperatures around the T_C. When the overall magnetization is less than 40% of the saturation magnetization (M_S), the MR in the paramagnetic phase shows excellent scaling with the square of the reduced magnetization following Eq. 2 (Fig. 2b), resulting in a scaling factor C of ~ 0.96. The quadratic dependence of MR on magnetization may suggest that magnetic scattering still plays an important role; however, in the spin scattering approximation, such a scaling ratio would correspond to a charge carrier density of about one per magnetic cell, which is an unlikely number for the exemplary Mott insulator because the $3d^1$ electrons of the V^{4+} ions are localized due to Coulomb interaction [51-54]. As we shall see, the effective carrier density at temperatures near the T_C determined by the HE measurements is only about 10^{17} cm^{-3}, which corresponds to a charge carrier to V^{4+} ion ratio on the order of 10^{-4} and a scaling factor of about 500 in Eq. 2. The substantial deviation of the scaling factor from the expected value implies that other unrevealed physical processes might be at work and compete with the electron-magnon interaction in $Lu_2V_2O_7$. However, the failure of the Majumdar-Littlewood model in the pyrochlore insulator cannot be attributed to the existence of itinerant charge carriers or lattice distortions as seen in the ferromagnetic semimetal EuB_6 [46] or lightly-doped mixed-valence manganites [47-50], respectively. Specifically, the room temperature resistivity value of $Lu_2V_2O_7$ is two orders of magnitude smaller than that of the undoped manganite $LaMnO_3$ [55], which may suggest an essential distinction in the electronic transport between the two materials.

It is interesting to note that the resistivity curve shown in the inset of Fig. 1a bears much resemblance to the temperature dependence of the resistivity of a lightly doped semiconductor, which is characterized by a metallic impurity-conduction regime separating the low-temperature impurity freeze-out range from the high-temperature intrinsic semiconductor transport [57]. In light of these remarkable similarities, investigations on the charge carrier density at different temperature and magnetic field conditions are particularly important to reveal the nature of electronic transport in the pyrochlore insulator $Lu_2V_2O_7$.

The most common route to the determination of the charge carrier density is through HE measurement [58]. For systems with a single type of charge carriers, the Hall resistivity depends linearly on the applied field and the slope reflects the sign and the density of charge carriers. However, the linear field dependence frequently breaks down for the Hall resistivity in multi-band materials due to the competition between different types of carriers [59]. In addition, spin dependent scattering in magnetic materials may also lead to a nonlinear HE which is described by [60]

$$\rho_H = R_n B + \mu_0 R_S M \tag{3}$$

where R_n is the ordinary Hall coefficient, B is the magnetic induction, and M is the magnetization. The second term, which becomes a constant as magnetization saturates, is known as the anomalous Hall effect (AHE). R_S is the AHE coefficient.

Fig. 3b shows the Hall resistivity curves of a $Lu_2V_2O_7$ single crystal at selected temperatures. The initial Hall coefficient is strongly temperature dependent. The sign of the zero-field Hall coefficient switches from positive to negative as temperature decreases, which indicates a change in the transport mechanism as the material enters the ferromagnetic phase. At temperatures around the T_C, the Hall resistivity curves always show a distinct slope change, even a sign reversal, with increasing magnetic field. Similar nonlinear HE at temperatures around T_C has been observed in a number of other magnetic materials [23-28]. Interestingly, the nonlinear HEs in these systems show a general feature, that is, the change in the Hall slope occurs at a constant magnetization far below the saturation magnetization at all temperatures [28]. In view of the magnetization curves shown in Fig. 3a, we confirmed that the switching point of each Hall resistivity curve (labeled by an arrow in Fig. 3b) indeed corresponds to a constant magnetization in the $Lu_2V_2O_7$ single crystal (indicated by a dashed line in Fig. 3a). This critical value is only about 40% of the saturation magnetization of the material, therefore the conventional mechanisms of the AHE [60], i.e. the skew scattering and the side-jump, are not responsible for the observed nonlinear HE. Interestingly, the critical magnetization coincides with the magnetization at which the MR begins to deviate from the quadratic scaling (Eq. 2). Similar coincidence has also been found in EuB_6 [28], where the critical magnetization is only about 10% of the saturation value. The fact that the similar coincidence in the two materials occurs at different critical magnetizations (respect to their own saturation values) suggests that the nonlinear HE and the deviation in MR are essentially related with each other and they may not be ascribed to exceeding the low-field limit [22]. In Ref. [28], a magnetization-driven percolative transition was proposed to explain the observed nonlinear HE as well as the MR in the ferromagnetic semimetal EuB_6: below a critical magnetization, carriers from some electronic bands are localized due to their strong interactions with local magnetic moments (formation of magnetic polarons); however, above the critical magnetization, an electronic percolative transition of these carriers associated with coalescence of magnetic polarons leads to a change in the effective carrier concentration and the Hall resistivity slope. According to this picture, it is the Hall resistivity slope ($d\rho_{xy}/dH$) instead of the Hall coefficient (ρ_{xy}/H) that reflects the competition of different types of carriers at high fields. Based on this picture, a two-component model was proposed to quantitatively describe the nonlinear HE [28],

$$\widetilde{R}(H,T) = R_0 f(H,T) + R_1 [1 - f(H,T)]$$

$$\text{with} \quad f(H,T) = \frac{1}{1+\exp[D(M-M_C)]} \tag{4}$$

where $\widetilde{R}(H,T) = d\rho_{xy}(H,T)/dH$ is the slope of the Hall resistivity at field H and temperature T, R_0 is the initial Hall coefficient, R_1 is the Hall resistivity slope at high fields, M is magnetization, M_C is the critical magnetization, and D is a constant reflecting the sharpness of transition.

As indicated by the solid curves in Fig. 3b, the highly nonlinear Hall resistivity of the $Lu_2V_2O_7$ single crystal at temperatures near the T_C is well reproduced by the two-component model using a single critical magnetization; at temperatures far above (120 K and 140 K) or below (58 K) the T_C the Hall resistivity is linear in the entire field range. The low-field and high-field Hall resistivity slopes determined from the simulations further allow us to quantitatively examine the change in the effective carrier density as a function of temperature and external magnetic field. At temperatures above the Curie temperature, the initial Hall coefficient (R_0) increases as temperature decreases, indicating a gradually decreasing effective carrier density. To test whether that the high-temperature activation behavior is due to intrinsic semiconductor transport because of the similarities mentioned above, we fit the temperature dependence of the effective carrier density to the activation equation for a semiconductor [57]

$$p_i = n_i = N_0 T^{3/2} \exp\left(\frac{-E_g}{2k_B T}\right) \tag{5}$$

where p_i and n_i are intrinsic carrier densities of holes and electrons, respectively; E_g is the semiconductor band gap; and N_0 is a constant. As shown in Fig. 4a, the initial Hall coefficients obtained in a temperature range from 76 K to 140 K can be described by the semiconductor activation model with an energy gap of 116 meV. However, according to previous theoretical and optical studies [51,52,56], this value is not only much smaller than the gap between the O 2*p* orbital and the upper Hubbard band but also one order of magnitude smaller than the Hubbard energy gap. With that considered, the small activation energy obtained in the material suggests that the high-temperature transport is probably not dominated by intrinsic charge carriers thermally excited across the semiconducting energy gap. However, the high-temperature transport mechanism in $Lu_2V_2O_7$ is also distinct from that in mixed-valence manganites where essentially hopping between Mn ions in different valence states is at work. As far as magnetic polaron hopping model is concerned, since some *n*-type carriers experience a delocalization process as the overall magnetization increases, these carriers are likely the *d*-band electrons which are strongly coupled with V^{4+} ions so that only hopping between isolated magnetic polarons is allowed at high temperatures. It has been observed that short-range magnetically ordered clusters are formed in the paramagnetic phase [60], confirming the presence of magnetic polarons in $Lu_2V_2O_7$ at high temperatures. However, as we have pointed out, magnetic polaron hopping model alone may not be able to provide full understanding of the high-temperature transport in $Lu_2V_2O_7$. In particular, no existing model could explain the failure of the Majumdar-Littlewood model in this stoichiometric pyrochlore system. A possible scenario to explain the observation is that other hopping mechanism such as Mott variable range hopping may also play a role. To completely clarify the activation mechanism at high temperatures, we believe that further studies especially by other experimental techniques are required.

The application of a magnetic field leads to the percolation of the magnetic polarons at the critical magnetization and the delocalization of charge carriers, resulting in the observed nonlinear HE. Consequently, the high-field Hall resistivity slope (R_1) reflects the competition between the delocalized charge carriers and the activation transport. The high-field Hall resistivity slope shows a nearly constant negative value over a temperature range from 76 K to 58 K (Fig. 3b), which strongly suggests the existence of donor impurities in the sample likely due to oxygen deficiency [62]. These impurity states are strongly correlated with V^{4+} ions thus experience a delocalization process with increasing magnetic field. To quantitatively describe the thermal evolution of the competition between the activation behavior and the impurity transport, we plot the high-field Hall resistivity slope as a function of the effective carrier density determined from the initial Hall coefficient in Fig. 4b. As the effective carrier density decreases to a very low level, the intercepted Hall resistivity slope corresponds to an electron impurity level of 8.8×10^{16} cm^{-3}. As the material enters the ferromagnetic phase, the impurity conduction gradually becomes the dominant component in the electronic transport, leading to the metallic-like transport behavior (Region B in the inset of Fig. 1). In the temperature range from 76 K to 58 K, the Hall resistivity slope remains unchanged at high magnetic field, which is consistent with the impurity-electron conduction scenario because the impurity level is determined in the synthesis process. When temperature decreases to below 40 K (Region C in the inset of Fig. 1a), the material enters another insulating regime. It has been reported that some pyrochlore systems also show an insulating ground state [63,64], which has been suggested to originate from the spin-ice state of these materials [65,66]. However, these models may not explain the observation here in $Lu_2V_2O_7$ because of the spontaneous ferromagnetism. In the case that impurity states are slightly below the electron band, they become only partially ionized when the Fermi level reaches the level at low temperatures, leading to the impurity freeze-out regime [57]. Within this picture, we found that the low-temperature electronic transport of $Lu_2V_2O_7$ can be well described by the Arrhenius behavior (n = 0 in Eq. 1), resulting in an ionization energy of ~ 7 meV (the inset of Fig. 1a). We also found that the impurity density (n^*) varies from sample to sample and the variation, as expected, leads to slightly different resistivity values in the metallic region (Region B); however, the activation laws for the high-temperature region (Region A) and for the low-temperature region (Region C) are quantitatively consistent in all the single crystals we studied.

In summary, to understand the complex properties of the ferromagnetic semiconductor $Lu_2V_2O_7$, we have systematically studied the interplay between the electronic transport and the magnetism. At temperatures near the T_C, the material shows a large negative magnetoresistance together with an unusual switch of the Hall resistivity slope in magnetic field. The nonlinear HE, which has also been observed in many other low-carrier-density ferromagnetic materials, provides clear evidence for a magnetization-driven percolative transition of charge carriers in $Lu_2V_2O_7$. However, analysis based on the magnetoresistance suggests that the magnetic polaron picture, which successfully explains the transport property of $Tl_2Mn_2O_7$ and many other ferromagnetic materials, does not fully account for the observations in $Lu_2V_2O_7$. Our studies suggest that competition between multiple hopping mechanisms may lead to the observed high-temperature activation behavior. Moreover, our quantitative analyses also indicate that the metallic electronic transport in the intermediate temperature range is dominated by impurity electrons which presumably come from oxygen deficiency in the material. In contrast to the low-temperature conducting behavior in mixed-valence manganites, $Lu_2V_2O_7$ shows a non-metallic ground state due to the freeze-out of the electron impurities.

Work at FSU was supported by NSF grants DMR-0908625 and DMR-1308613. C. W. is supported by NSERC, the CRC program (Tier II), and CFI.

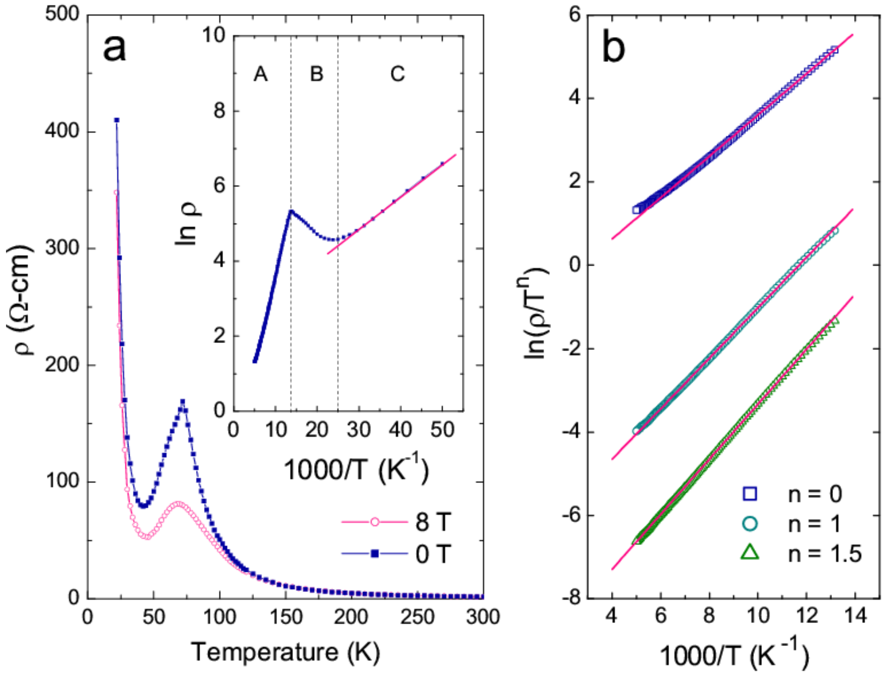

FIG. 1. (Color online) a) Temperature-dependent resistivity measured at zero field (blue) and 8 T (red). The inset indicates that the temperature dependence is consisted of two activated regions (A and C) separated by a metallic-like temperature range (B). Solid line in the inset is a fit to the simple activation law (Eq. 1) for the low-temperature resistivity. b) The resistivity curve in a temperature range from 75 K to 200 K is fitted to Eq. 1 with *n* = 0 for the Arrhenius activation model, *n* = 1 for the adiabatic small magnetic-polaron hopping model, and *n* = 3/2 for the non-adiabatic small magnetic-polaron hopping model.

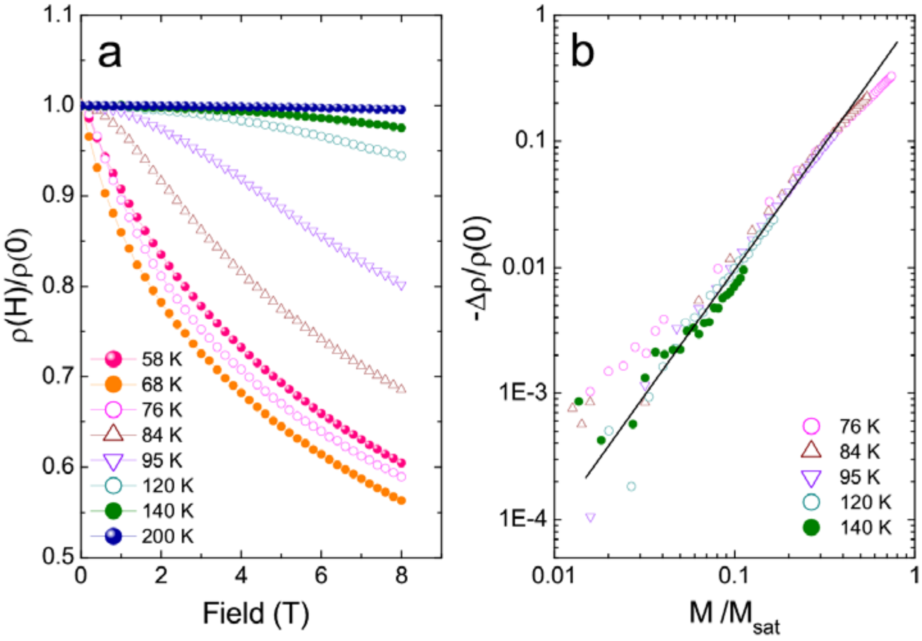

FIG. 2. (Color online) a) The normalized resistivity of $Lu_2V_2O_7$ as a function of external magnetic field at selected temperatures. b) log-log plot of the MR versus with the reduced magnetization at temperatures above the T_C, which shows a power-law scaling following Eq. 2.

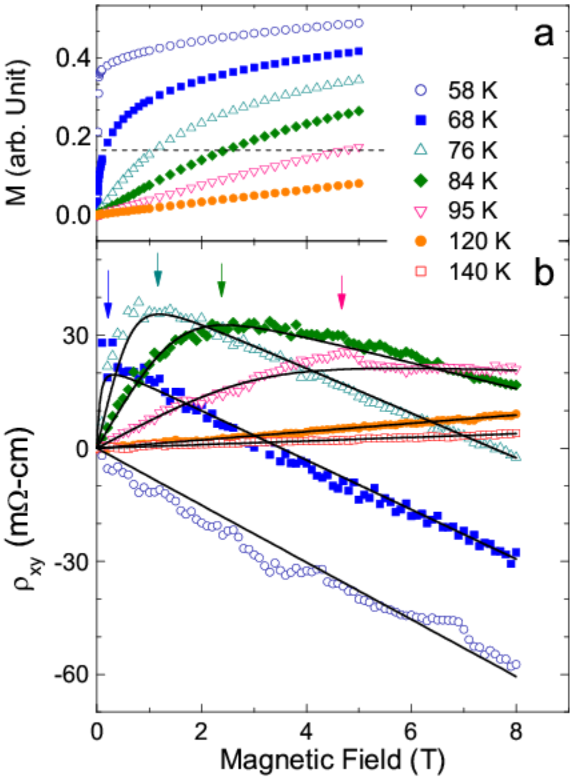

FIG. 3. (Color online) Magnetization a) and Hall resistivity b) of $Lu_2V_2O_7$ at selected temperatures. Solid curves in b) are the best fits of the Hall resistivity curves based on either linear dependence (for T = 140 K, 120 K, and 50 K, temperatures much above or below T_C) or the two-component model, Eq. 4 (for T = 95 K, 84 K, 76 K, and 68 K, temperatures near T_C). For each nonlinear Hall resistivity curve, an arrow is used to indicate the field position where the Hall resistivity slope changes. The dashed line in a), representing a constant magnetization, intercepts each curve at a magnetic field consistent with that indicated by the corresponding arrow in b), which suggests that the change in the Hall resistivity slope occurs at the same characteristic magnetization.

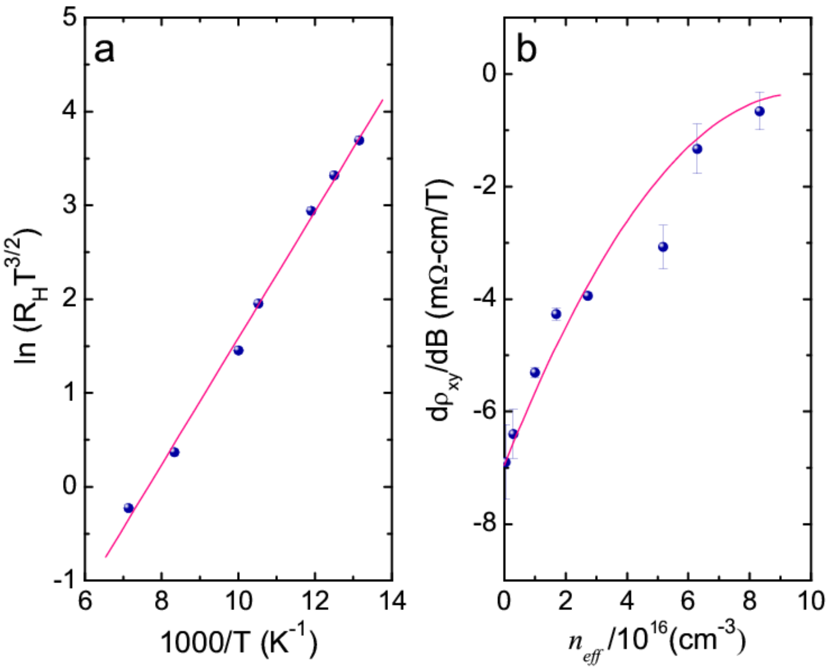

FIG. 4. (Color online) a) The temperature dependence of the zero-field Hall coefficient of $Lu_2V_2O_7$. The solid line is the best fit to the intrinsic semiconductor activation behavior (Eq. 5); b) High-field Hall resistivity slope as a function of the effective carrier density calculated from the zero-field Hall coefficient at the same temperature. The solid curve is to guide eye. The results suggest the presence of electron donor impurities possibly due to an oxygen deficiency.

REFERENCES

[1] R. Moessner and A. P. Ramirez, Phys. Today **59**, 24 (2006).

[2] J. E. Greedan, J. Alloys Compd. **408**, 444 (2006).

[3] M. J. Harris, S. T. Bramwell, D. F. McMorrow, T. Zeiske, and K. W. Godfrey, Phys. Rev. Lett. **79**, 2554 (1997).

[4] A. P. Ramirez, A. Hayashi, R. J. Cava, R. Shiddharthan, and B. S. Shastry, Nature (London) **399**, 333 (1999).

[5] S. T. Bramwell and M. J. P. Gingras, Science **294**, 1495 (2001).

[6] Y. Taguchi, Y. Oohara, H. Yoshizawa, N. Nagaosa, Y. Tokura, Science **291**, 2573 (2001).

[7] S. Onoda and N. Nagaosa, Phys. Rev. Lett. **90**, 196602 (2003).

[8] Y. Machida, S. Nakatsuji, Y. Maeno, T. Tayama, T. Sakakibara, and S. Onoda, Phys. Rev. Lett. **98**, 057203 (2007).

[9] D. J. P. Morris, D. A. Tennant, S. A. Grigera, B. Klemke, C. Castelnovo, R. Moessner, C. Czternasty, M. Meissner, K. C. Rule, J.-U. Hoffmann, K. Kiefer, S. Gerischer, D. Slobinsky, and R. S. Perry, Science **326**, 411 (2009).

[10] T. Fennell, P. P. Deen, A. R. Wildes, K. Schmalzl, D. Prabhakaran, A. T. Boothroyd, R. J. Aldus, D. F. McMorrow, and S. T. Bramwell, Science **326**, 415 (2009).

[11] M. A. Subramanian, B. H. Toby, A. P. Ramirez, W. J. Marshall, A. W. Sleight, and G. H. Kwei, Science **273**, 81 (1996).

[12] Y. Shimakawa, Y, Kubo, and T. Manako, Nature **379**, 53 (1996).

[13] J. M. D. Coey, M. Viret, and S. von Molnár, Adv. Phys. **48**, 167 (1999).

[14] M. B. Salamon and M. Jaime, Rev. Mod. Phys. **73**, 583 (2001).

[15] E. Dagotto, T. Hotta, and A. Moreo, Phys. Rep. **344**, 1 (2001).

[16] K. Yosida, Phys. Rev. **107**, 396 (1957).

[17] N. Furukawa, J. Phys. Soc. Jpn. **63**, 3214 (1994).

[18] Y. Tokura, A. Urushibara, Y. Moritomo, T. Arima, A. Asamitsu, G. Kido, N. Furukawa, J. Phys. Soc. Jpn. **63**, 3931 (1994).

[19] K. Kubo and N. Ohata, J. Phys. Soc. Jpn. **33**, 21 (1972).

[20] N. Furukawa, J. Phys. Soc. Jpn. **64**, 2734 (1995).

[21] P. Majumdar and P.B. Littlewood, Phys. Rev. Lett. **81**, 1314 (1998).

[22] P. Majumdar and P.B. Littlewood, Nature **395**, 479 (1998).

[23] H. Imai, Y. Shimakawa, Yu. V. Sushko, and Y. Kubo, Phys. Rev. B **62**, 12190 (2000).

[24] Y. Lyanda-Geller, S. H. Chun, M.B. Salamon, P. M. Goldbart, P. D. Han, Y. Tomioka, A. Asamitsu, and Y. Tokura, Phys. Rev. B **63**, 184426 (2001).

[25] H. C. Yang, L. M. Wang, H. E. Horng, Phys. Rev. B **64**, 174415 (2001).

[26] S. H. Chun, M. B. Salamon, and P. D. Han, Phys. Rev. B **59**, 11155 (1999).

[27] X. H. Zhang, S. von Molnár, Z. Fisk, and P. Xiong, Phys. Rev. Lett. **100**, 167001 (2008).

[28] X. H. Zhang, L. Q. Yu, S. von Molnár, Z. Fisk, and P. Xiong, Phys. Rev. Lett. **103**, 106602 (2009).

[29] L. Q. Yu, L. F. Wang, X. H. Zhang, W. B. Wu, S. von Molnár, Z. Fisk, and P. Xiong, New J. Phys. **15**, 113057 (2013).

[30] H. D. Zhou, E. S. Choi, J. A. Souza, J. Lu, Y. Xin, L. L. Lumata, B. S. Conner, L. Balicas, J. S. Brooks, J. J. Neumeier, and C. R. Wiebe, Phys. Rev. B **77**, 020411(R) (2008).

[31] M. Jaime, H. T. Hardner, M. B. Salamon, M. Rubinstein, P. Dorsey, an D. Emin, Phys. Rev. Lett. **78**, 951 (1997).

[32] G. Jakob, W. Westerburg, F. Martin, and H. Adrian, Phys. Rev. B **58**, 14966 (1998).

[33] S. H. Chun, M. B. Salamon, Y. Tomioka, Y. Tokura, Phys. Rev. B **61**, R9225 (2000).

[34] D. C. Worledge, G. J. Snyder, M. R. Beasley, T. H. Geballe, R. Hiskes, and S. DiCarolis, J. Appl. Phys. **80**, 5158 (1996).

[35] A. Banerjee, S. Pal, E. Rozenberg, and B. K. Chaudhuri, J. Phys.: Condens. Matter **13**, 9489 (2001).

[36] J. Lago, P. D. Battle, M. J. Rosseinsky, A. I. Coldea, and J. Singleton, J. Phys.: Condens. Matter **15**, 6817 (2003).

[37] N. Nakamura and E. Iguchi, J. Solid State Chem. **145**, 58 (1999).

[38] W.-H. Jung, H. Wakai, H. Nakatsugawa, and E. Iguchi, J. Appl. Phy. **88**, 2560 (2000).

[39] M. Rubinstein, D. J. Gillespie, J. E. Snyder, and T. M. Tritt, Phys. Rev. B **56**, 5412 (1997).

[40] S. von Molnar and S. Methfessel, J. Appl. Phys. **38**, 959 (1967).

[41] C. Haas, A. M. J. G. van Run, P. F. Bongers, and W. Albers, Solid State Commun. **5**, 657 (1967).

[42] A. P. Ramirez, R. J. Cava, and J. Krajewski, Nature **386**, 156 (1997).

[43] R. W. Cochrane, F. T. Hedgcock, J. O. Ström-Olsen, Phys. Rev. B **8**, 4262 (1973).

[44] S. Yamaguchi, H. Taniguchi, H. Takagi, T. Arima, and Y. Tokura, J. Phys. Soc. Jpn. **64**, 1885 (1995).

[45] B. Martínez, J. Fontcuberta, A. Seffar, J. L. García-Muñoz, S. Piñol, and X. Obradors, Phys. Rev. B **54**, 10001 (1996).

[46] S. Süllow, I. Prasad, S. Bogdanovich, M. C. Aronson, J. L. Sarrao, and Z. Fisk, J. Appl. Phys. **87**, 5591 (2000).

[47] A. P. Ramirez, J. Phys.: Condens. Matt. **9**, 8171 (1997).

[48] A. J. Millis, P. B. Littlewood, and B. I. Shraiman, Phys. Rev. Lett. **74**, 5144 (1995).

[49] H. Roder, J. Zang, and A. R. Bishop, Phys. Rev. Lett. **76**, 1356 (1996).

[50] A. J. Millis, B. I. Shraiman, and R. Mueller, Phys. Rev. Lett. **77**, 175 (1996).

[51] H. J. Xiang, E. J. Kan, M.-H. Whangbo, C. Lee, S. H. Wei, and X. G. Gong, Phys. Rev. B **83**, 174402 (2011).

[52] S. Shamoto, H. Tazawa, Y. Ono, T. Nakano, Y. Nozue, T. Kajitani, J. Phys. Chem. Solids **62**, 325 (2001).

[53] H. Ichikawa, L. Kano, M. Saitoh, S. Miyahara, N. Furukawa, J. Akimitsu, T. Yokoo, T. Matsumura, M. Takeda, and K. Hirota, J. Phys. Soc. Jpn. **74**, 1020 (2005).

[54] A. A. Biswas and Y. M. Jana, J. Magn. Magn. Mater. **329**, 118 (2013).

[55] A. Urushibara, Y. Moritomo, T. Arima, A. Asamitsu, G. Kido, and Y. Tokura, Phys. Rev. B **51**, 14103 (1995).

[56] S. Yamanouchi, Y. Okimoto, Y. Taguchi, T. Katsufuji, Y. Tokura, Part 3, Meet. Abstr. Phys. Soc. Jpn 53-1 (1998) 617 (2a-R-9).

[57] B. I. Shklovskii and A. L. Efros, *Electronic Properties of Doped Semiconductors* (Springer-Verlag, Berlin Heidelberg, 1984).

[58] C. L. Chien and C. R. Westgate, *The Hall Effect and Its Applications* (Plenum Press, New York, 1980).

[59] S. M. Watts, S. Wirth, S. von Molnár, A. Barry, and J. M. D. Coey, Phys. Rev. B **61**, 9621 (2000).

[60] N. Nagaosa, J. Sinova, S. Onoda, A. H. MacDonald, and N. P. Ong, Rev. Mod. Phys. **82**, 1539 (2010).

[61] K.-Y. Choi, Z. Wang, P. Lemmens, H. D. Zhou, J. van Tol, N. S. Dalal, and C. R. Wiebe, Phys. Rev. B **82**, 054430 (2010).

[62] G. T. Knoke, A. Niazi, J. M. Hill, and D. C. Johnston, Phys. Rev. B **76**, 054439 (2007).

[63] S. Nakatsuji, Y. Machida, Y. Maeno, T. Tayama, T. Sakakibara, J. van Duijn, L. Balicas, J. N. Millican, R. T. Macaluso, and J. Y. Chan, Phys. Rev. Lett. **96**, 087204 (2006).

[64] S. M. Disseler, C. Dhital, T. C. Hogan, A. Amato, S. R. Giblin, C. de la Cruz, A. Daoud-Aladine, S. D. Wilson, and M. J. Graf, Phys. Rev. B **85**, 174441 (2012).

[65] M. Udagawa, H. Ishizuka, and Y. Motome, Phys. Rev. Lett. **108**, 066406 (2012).

[66] G.-W. Chern, S. Maiti, R. M. Fernandes, and P. Wölfle, Phys. Rev. Lett. **110**, 146602 (2013).